Middle-Atmosphere Temperature Monitoring Addressed with a Constellation of CubeSats dedicated to Climate issues

Philippe Keckhut, Alain Hauchecorne, Mustapha Meftah, Sergey Khaykin, Chantal Claud, Pierre Simoneau

Middle-Atmosphere Temperature Monitoring Addressed with a Constellation of Cube-Sats dedicated to Climate issues

Philippe Keckhut*, Alain Hauchecorne, Mustapha Meftah, Sergey Khaykin

LATMOS/IPSL, UVSQ, Université Paris-Saclay, Sorbonne Université, CNRS/INSU, Guyancourt, France

Chantal Claud

Laboratoire de Météorologie Dynamique, Ecole Polytechnique, CNRS/INSU, Palaiseau, France

Pierre Simoneau

ONERA, Chemin de la Hunière, Palaiseau, France

Corresponding author: Philippe Keckhut, keckhut@latmos.ipsl.fr

ABSTRACT

While meteorological numerical models extend upward to the mesopause, mesospheric observations are required for leading simulations and numerical weather forecasts and climate projections. This work reviews some of the challenges about temperature observation requirements and the limiting factors of the actual measurements associated with atmospheric tides. A new strategy is described here using the limb scattering technique based on previous experiments in space. Such observations can be placed on board cube-satellites. Technical issues are the large dynamic range (4 magnitudes) required for the measurements, the accuracy of the limb pointing and the level of stray light. The technique described here will expect accuracy of 1-2 K with a vertical resolution of 1-2 km. A constellation of 100 platforms could provide temperature observations with space (100 km) and time resolution (3 hours) recommended by the World Organization Meteorology, while tidal issues could be resolved with a minimum of 3-5 platforms with specific orbit maintained to avoid drifts.

1. Introduction

The middle atmosphere (MA) is under the conjugated influence of climate changes, due to anthropogenic activities and natural variability. This region exhibits variability on time and space with scales ranging from thousands of kilometers to tens of meters and extending in the different atmospheric layers from troposphere up to the lower thermosphere. The MA extends from the tropopause (10-15 km) to the turbopause (100-105 km) comprising the stratosphere and mesosphere (Blanc et al. 2017). The stratosphere (12-50 km) was extensively studied because of the ozone hole discovery (Farman et al. 1985) and the associated cooling due to the strong temperature-ozone dependence in the upper stratosphere. The increase of GHGs (Green House Gases) induces a global warming at the surface and in the troposphere but also a global cooling in the MA due to the thermal infrared radiation emitted by GHGs escaping directly to the space because of the low optical thickness of the atmosphere above. However, full interactive numerical models including the MA have only appeared since the 1990s (Rind et al. 1990). The Coupled Model Inter-comparison Project reveals that models that do not represent the MA present biases in the representation of stratospheric climate and variability (Charlton-Perez et al. 2013). For this reason, the European Center for Medium range Weather Forecast (ECMWF) extends meteorological analyses up to the mesopause (80 km). However, comparisons between meteorological analyses and ground-based instrument reveal large biases (Le Pichon et al. 2015; Wright and Hindley 2018) that are due to a critical lack of observations above the stratopause and deficiencies in the parametrization of radiation as well as gravity wave effects in assimilating models. Limb missions, providing atmospheric observations with a high vertical resolution, will all stop soon their operations (Fussen et al. 2019). Apart from ISS/SAGE-III launched in 2016, only few limb scattering missions are planned in the future while they are not specifically dedicated to temperature retrieval. Long-term

temperature evolutions in the mesosphere (Beig et al. 2003) also suffer from the lack of dedicated observations (section 2). However limb viewing observations allows temperature retrieval with a good vertical resolution and can be deployed on small satellites (section 3). An issue is related to the fact that temperature observations exhibit strong interferences with tides as described in section 4. The concept of constellation of several cubesats as described in section 5 could be an interesting approach to provide unbiased mesospheric temperature fields for models. Section 6 will provide conclusions about such perspectives.

2. Middle Atmosphere Temperature Variability

Systematic global temperature observations from space were initiated since October 1978 with the SSU (Stratospheric Sounding Unit) onboard the successive NOAA operational satellites (Gelman and Nagatani 1977) while assimilation of SSU data begins in December 1978 in ERA5. After adjustments with rockets (Gelman et al. 1986) continuous temperature series were derived by the U.S. National Centers for Environmental Prediction (NCEP), and decadal temperature trends were estimated (Hood et al. 1993; Lambeth and Callis 1994) with large uncertainties due to adjustment uncertainties between the successive satellites (Wild et al. 1995). The updated temperature series by two different groups show that derived trends exhibit larger differences between both of them than with temperature series provided by numerical models (Thompson et al. 2012) and finally provide a better agreement on zonal series (Maycock et al. 2018). A new generation of stratospheric temperature sounders were obtained with the Advanced Microwave Sounding Unit (AMSU) on board successive NOAA satellites and have also been flown more recently on NASA/Aqua and EUMETSAT/Metop satellites. The overlap periods reveal bias and drifts (Keckhut et al. 2015) in agreement with tidal models indicating that most of the observed drifts are likely due to the atmospheric tides. Atmospheric tides are caused by a combined effect of ozone and water vapor

photodissociation (Haefele et al. 2008) and insolation absorption by these same species, inducing waves with periods of 24 hours and associated harmonics on dynamical parameters (temperature, wind and pressure) that propagate in the whole atmosphere(Chapman and Lindzen 1970). The difficulties about time continuity on both SSU and AMSU series are mainly due to the combined effects of satellite orbit, atmospheric tides, and differences in weighting functions (Figure 1). With temperatures from the AQUA/AMSU instrument having an orbit maintained, more accurate trends can be obtained (Funatsu et al. 2016; Khaykin et al. 2017a). While trend analyses are very sensitive to time and space sampling (Funatsu et al. 2011), observations need to continue over periods longer than one solar cycle. However, tide characteristics may also change in response to climate change inducing additional apparent trends (Morel et al. 2004). AMSU has a finer vertical resolution than SSU but sounds not as high as SSU (Zou and Qian 2016). Mesospheric temperature was first investigated by rocketsondes operated systematically since the 1960s up to the end of the 1980s. Since then, observations have been performed with lidars within the NDSC network (Kurylo 1991) at several sites from tropics to poles. In the upper mesosphere temperature data are also obtained from airglow OH spectrometers (Bittner et al. 2002). In addition, few other research instruments have provided multi-years temperature data, and trends have been derived by several groups (Beig et al. 2003). These observations are consolidated and coordinated through the ARISE project (Blanc et al. 2017). No operational satellites are dedicated to provide systematic mesospheric temperatures. Some research satellites like the HALOE experiment aboard UARS provide multi-year observations using the solar occultation technique (Remsberg et al. 2002) with a good vertical resolution. However, no successive similar instruments were planned to be launched soon to ensure the continuity. At that time, only two research satellites provide continuing temperature series in the mesosphere: MLS (Microwave Limb Sounder) on board AURA/NASA and SABER (Sounding of the Atmosphere using Broadband Emission Radiometry) on board TIMED/NASA

(Thermosphere Ionosphere Mesosphere Energetics Dynamics). Large bias with ground-based observations are reported (Wing et al. 2018), and no similar follow-up missions are planned. Microwave instruments like MLS do not exhibit a good vertical resolution with typical values of 8 km at 30 km growing with altitude up to 14 km at 80 km, and are then not sensitive enough to reveal disturbances like mesospheric inversions. Instruments like SABER provides more information in the mesosphere/thermosphere region with a constant vertical resolution of around 2 km. In the MA, short scale processes like gravity waves are fundamental to understand atmospheric evolution like sudden stratospheric Warmings (Hauchecorne et al. 2019a; Noguchi et al. 2020) and cannot be vertically resolved by operational sensors (Figure 1). Comparison with numerical weather model shows that under 10 days part of the observed variability is not included in meteorological analyses (Le Pichon et al. 2015). The variability in the mesosphere is also due to gravity waves breaking leading to mesospheric inversions of several tens of degrees within a vertical layer of 10-20 km (Hauchecorne et al. 1987). Such structures are already observed from space (Leblanc et al. 1995) and modelled (Hauchecorne and Maillard 1990) and were detected also by GOMOS (Hauchecorne et al. 2019a). The role of the mesospheric and upper stratospheric circulations appear to be critical on the onset and development of SSWs (Charlton-Perez et al. 2013).

The observation requirements are compiled by World Meteorological Organization (WMO) through the Observing Systems Capability Analysis and Review Tool (OSCAR: www.wmo-sat.info/oscar). The target resolutions correspond to 50-100 km and 3-6 hours time-resolution with an accuracy of 1-2 K.

3. Limb viewing measurements from small satellites

The scattering of sunlight is only due to atmospheric molecules above the aerosol stratospheric layer (25-30 km) and when no high-altitude polar clouds are present (Polar Stratospheric or

Mesospheric Clouds). Since Lord Rayleigh, the scattering is known to have a better higher efficiency for the shorter wavelengths revealing a blue scattering (Figure 2). This scattering is directly proportional to the atmospheric density.

Thus, similarly to the lidar technique (Hauchecorne and Chanin 1980), temperature can be retrieved by downward integration of the hydrostatic equation assuming the atmosphere follows the perfect gas law. The initialization is performed at the top of the profile assuming that the temperature is close to the climatology. The associated uncertainty is decreasing rapidly with altitude because the density itself increases sharply and the error becomes rapidly negligible providing an unbiased absolute temperature profile in the whole MA. This method has been first applied from space on bright limb using the Solar Mesosphere Explorer (Clancy et al. 1994). The similar retrieval was applied on space experiments that were not initially planned to provide temperatures like WINDII on UARS (Shepherd et al. 2001), OSIRIS on Odin (Sheese et al. 2012) and more recently with GOMOS on ENVISAT (Hauchecorne et al. 2019b) but having a limb viewing geometry. The temperature retrievals were validated by ground-based instruments showing very accurate unprecedent observations in the mesosphere with agreement better than 2K with a vertical resolution of 2km. While existing instrument in space shows great capabilities, the development of a dedicated instrument appears to be feasible as it could be integrated on a small platform. Similar strategy have already be proposed for Earth radiative balance (Meftah et al. 2020) for other essential climate variable. Such an instrument requires to observe the bright limb, and make the image of the Limb (Figure 3) on a CCD sensor. The main difficulties consist in:

- tracking the limb with a good accuracy,

- being sensitive to a large dynamic signal while density is decreasing by two magnitudes from 30-80 km and

- fully eliminating parasitic lights from Earth surface and internal glint.

To achieve an accuracy of 1 K, a pointing reliability better than 250 meters is required as the mean temperature gradient in the mesosphere corresponds to 4K/km. For the pointing, if we consider a satellite cruise altitude of 600 km and a tangent altitude at 65 km above the surface, the distance to the limb is 2678 km. An accuracy of 200 meters corresponds to 70 microradians (or 15 arcsec). With GOMOS such accuracy was ensured with an efficient star tracker (Bertaux et al. 2010), while the occultation method requires to track a star through the different atmospheric layers during the satellite course. Similar device is required for temperature observations but with lower capability requirements as we only need to retrieve 200 m resolution (15 arcsec) in one exposure time. While the room is limited in a Cube-Sat, if the pointing efficiency is not as good as expected, the altitude can be also derived directly from the image of the horizon observed on the full multi-point detector. Such concept avoids to scan the limb in order to retrieve the density profile with a mechanic system and provide an altitude reference in detecting the Earth horizon. The main challenge with such a detector consists in providing enough sensitivity with a small noise level, over a signal range covering more than 4 magnitudes (Figure 4). Simulations of expected limb radiances have been performed for several bands and Figure 4 exhibits the two bands selected. It shows that whatever the wavelength, the signals should cover four orders of magnitude. The blue part of the spectrum is optimum as it is not affected by any absorbing component. Since the temperature retrieval requires a pure molecular scattering, the red part of the spectrum, more sensitive to the particulate scattering, will be used to detect the presence of aerosol and cloud particles. Even though the MA is mostly free of particulates, moderate volcanic eruptions or intense biomass burning events can inject considerable amounts of aerosols into the stratosphere (Khaykin et al. 2017b, 2020). Additionally, high-altitude tropical cirrus clouds, polar winter stratospheric clouds

as well as mesospheric noctilucent clouds or meteorite showers can also contaminate molecular scattering. The detection of aerosol and clouds using limb scattering technique will be the subject of a different study. Multi-point detectors exhibit different characteristics in term of sensitivity response and noise level as observed on GOMOS detector (Keckhut et al. 2010). Altitude retrieval will require an accurate inter-pixel calibration (0,5) as performed on GOMOS for spectrum retrieval (Kyrola et al. 2010). The calibration issue will be the task of the coming tests with the instrument prototype.

Another important issue is related to the noise induced by the external stray light reaching the detector. It appears that some light outside the nominal field of view of the instrument was observed on the GOMOS instrument (Figure 5) analyses on Envisat (Kyrola et al. 2010). Such noise reduce the altitude range. Part of the light can be scattered by some platform hardware into the baffle and optics. The other part is coming from the sun-illuminated nadir. Noise can be estimated directly from signals coming from altitudes above 100 km, however capability will be increased if the noise effects could be reduced by the design of the instrument. The dynamic and level of noise will allow to select the correct 2D multi-pixel detector. If no active thermal control on board is planned, power consumption will fit with a 3U (6W) or 6U (15W) standard orbit average power available. An accurate characterization of the dark current with temperature and data processing need to be performed at ground. All the components of similar limb measurements have already operated in space through instruments mentioned above. So the technical challenge consists today in performing similar measurements on a small platform with reduced room, electrical power, and weight. To achieve the 3 main technical issues described in section 3, nano-satellite pointing devices qualified for nanosat are not numerous but one has already shown promising capabilities (Mason et al. 2017) that need to be investigated further for our application. The dynamic of the signal can be covered by a CCD sensor while design, simulations and tests will be conducted

to reduce strait light issues on a small platform. Observation geometry as well as illumination conditions will not change during temperature observations that should reduce large evolution of the noise from successive observations. At that time a prototype with a flexible setup is under study and coming measurement campaigns in a high altitude observatory will allow for a better assessment of the noise and adjustment of the final design including the potential inclusion of foldable baffle.

4. Tidal issues

Atmospheric tidal theory has been proposed by Chapman and Lindzen (1970) predicting a zonally-invariant migrating mode (Sun-synchronous) and a zonally-variant non-migrating tide. The atmospheric tides are primarily induced by the daytime heating of stratospheric ozone layer and convective latent heat release in the upper troposphere, whereas the ozone and water vapor are themselves subject to a strong diurnal cycle due to the photodissociation effect (Haefele et al. 2008). Perturbations of dynamical parameters like temperature and wind propagate vertically throughout the different atmospheric layers up to the thermosphere, and their amplitudes grow with decreasing pressure due to energy conservation.

Until recently, only few observations of tides in the stratosphere were available. Tidal studies in this layer have thus been restricted almost exclusively to rocket soundings. Rocket-borne temperature measurements had sparse diurnal coverage and were also prone to errors induced by radiation from exposed components of the rocketsonde (Finger and H.M. 1967; Hoxit and Henry 1973). Atmospheric tides from temperature satellite measurements have been obtained from different space instruments (Raju et al. 2010): LIMS (Limb Infrared Monitor of the Stratosphere) instrument aboard the Nimbus7 (Hitchman and Leovy 1985), ISAMS (Improved Stratospheric and Mesospheric Sounder)and MLS (Microwave Limb Sounder) instruments aboard the Upper

Atmosphere Research Satellite (Dudhia et al. 1993; Keckhut et al. 1996), and more recently from CRISTA mission (Ward et al. 1999; Oberheide and Gusev 2002). However, satellite radiometers need systematic validations and periodic calibrations by ground references and observations are impeded with low horizontal and vertical resolutions and a viewing window that limits the local time of observations. The analyses of daily-scale atmospheric fluctuations associated for example with planetary waves are potentially contaminated by the non-migrating diurnal tides. The distortion in the analysis of planetary waves due to the tidal contamination was found to be of the same magnitude to the impact of noise in the data averaging over space and time (Zhang et al. 2006). The diurnal solar tide is one of the most prominent features in the middle atmosphere. While the tidal effect on large-scale stratospheric dynamics is small, its representation in a model is important for data assimilation in order to avoid introducing biases associated with the local time of the measurements (Swinbank and O'Neill 1994; Swinbank et al. 1999). This issue is much more critic in the mesosphere where the tidal amplitude is nearly a magnitude larger. Data processing from a single satellite requires large assumption about tidal characteristics (Huang et al. 2010). The tide is also modulated by ozone, water vapor density and by the dynamic (McLandress 2002), thus is sensitive to inter-annual changes like the QBO and SAO. Numerical simulations reveal a high sensitivity and expect tides characteristics to vary with climate changes (Morel et al. 2004). Thus simultaneous tidal estimates are required for assimilation or comparisons of any measurements performed at different time of the day. One shortcoming of the satellite mesospheric temperature data is that they are biased by the presence of migrating tides depending on the local times at which the daily zonal mean temperatures are obtained. No single satellite is able to provide a full diurnal coverage above a given location. At best if we consider a long period, the orbit changes allow to sample different parts of the diurnal cycle permitting the derivation of mean tidal information in comparing with temperatures at fix given times given by operational NOAA satellites. This is the

case for UARS/MLS (Keckhut et al. 1996) and SABER that obtained a full 24-hour coverage in respectively 36 and 60 days. However tidal retrievals are biased by the daily variability (Forbes and Wu. 2006). For WINDII only daytime observations are obtained and the diurnal tide parameters (amplitudes and phases) cannot be determined without some assumptions about phase information. This issue is a strong limitation for waves with period greater than 2 days, because of aliasing effects with this tidal periods. In the mesosphere, ERA interim model, which provides data every 6 hours, allow us to derive a diurnal cycle in assuming no semi-diurnal component and only a diurnal one (Figure 6). This calculation average over one month reveals at 60 km a large difference with latitudes but also unexpected large differences along the longitudes because of the strong presence of non-migrating tides. Complementary analyses with superDARN radar reveal a large variability of tides in wind with time and even over a single latitude (Hibbins et al. 2019).

5. Small-satellite strategy, stable orbit and constellations

The orbit needs to be selected to see an illuminated limb. In the summer hemisphere, above 30 km, a large portion of the diurnal cycle is concerned (more than 15 hours at 45° in latitude) while in the winter hemisphere a reduced portion is available (less than 10 hours at 45° in latitude). If most of the variability induced by migrating atmospheric tides can be modelled by a diurnal and a semi-diurnal components, 5 unknown variables need to be considered (amplitude and phase for both waves and the mean). Temperature time evolution induced by tides are provided by the Global Wave Scale Model (Hagan 1999). If we consider a noise of 2K at 65 km at mid-latitudes with 5 different solar times and 30 observations (corresponding to 1 month daily measurements), the retrieval of the tidal evolution is perfectly reproduced (deviations smaller than 5% over the full cycle) as shown in figure 7. If the satellite has two solar time observations for respectively ascending and descending orbits, then only 3 satellites are necessary to retrieve atmospheric tides. During winter, the night is

too long to provide a sufficient coverage to retrieve the full characteristics of tidal waves (Figure 7). Figure 7 clearly shows how crucial are the observations at around 19:00 to retrieve the amplitude of tides as this portion of the cycle exhibits the largest differences between December and August tidal behaviors. So, the 3 solar-time observations are enough to retrieve the daylight portion of the temperature daytime evolution. However, orbits of the different satellites need to be decided accurately to remove tide effects if only 3 platforms are in space. One of the important issues to time continuity, consists in maintaining the orbit stable in time while a drift would induce change of the time of measurements. Due to the atmospheric tides inducing several-degrees temperature oscillations in the middle atmosphere, the drift about the revisiting time over a given location, will induce a temperature drift that could be interpreted either as anthropogenic trend or instrumental drift. As discussed in section 2, tides have been already observed with operational instruments like SSU (Wild et al. 1995) and AMSU (Keckhut et al. 2015) and were a severe limitation for trend estimates, unless the instruments have been installed on platforms with stable orbits (Funatsu et al. 2016). Small thrusters have been developed for Cube-Sats and can be used to maintain the time of measurements. If many satellites are in space simultaneously the maintenance of the orbit is not required in theory. However, while it is miniaturized and recommended for de-orbitation and collision avoidance such a device will present a plus-value for trend retrieval using a reduced number of platforms.

However, such temporal sampling should be considered as a minimum requirement to address tidal issues as only migrating time were considered. Very few is known about non-migrating tides and it is difficult to plan specific operations. WMO requirements will certainly allow a better representation of the induced regional effects. In order to achieve the required resolution provided by OSCAR/WMO during daytime with Low Earth Orbit (LEO) satellites, 4 orbital planes with a 3-hours offset between them are needed, for example at 7:30, 10:30, 13:30 and 16:30 local time

(Thompson et al. 2012). To achieve the horizontal resolution of 100 km for each orbit plane, 400 longitudes are needed at the equator. With up to 16 orbits per day for a LEO satellite, 25 platforms are needed on each orbit plane, corresponding to a total of 100 platforms.

Due to the agility of CubeSats, an international collaborative heterogeneous constellation can be envisioned to detect and study global dynamical structures in the MLT region using deep learning approaches as already suggested (Kaufmann et al. 2018; Meftah et al. 2020). Heterogeneity can come from limb scattering platforms like the one introduced here with additional capabilities or other limb-viewing instruments not primarily designed for temperature retrieval like ALTIUS (Fussen et al. 2019) or OMPS-LP on JSPS, or even measurements based on other techniques that provide observations on the dynamics in the MA (Baron et al. 2018; Fussen et al. 2019).

6. Conclusions and recommendations

Previous studies have revealed difficulties to derive temperature trends in the upper stratosphere with successive operational instruments with different orbits and/or having experienced orbit drifting in time due to tidal effects. Tidal issue is also limiting the assimilation processes in meteorological analyses. Moreover in mesosphere, where tidal amplitudes are much larger, temperature is only probed by few research satellites and requires a better observation strategy. To insure a good time temperature coverage of the upper stratosphere and mesosphere to avoid interferences with tides, several orbits are required, ideally more than 5 as shown by simulations described in section 5. Ideally, process studies would require around 100 platforms. This can not insure with traditional space platforms. While climate variables are linked together and is required to quantify and understand the Earth imbalance, different constellations will be merged together with artificial intelligence methods. Temperature observations should be performed with a noise smaller than 1-2 Kelvin, and a systematic bias even smaller by 2 magnitudes. Previous

temperature retrievals from limb scattering appear to be one of the best technologies to provide accurate temperatures with a simple concept that can fit a small satellite platform, adequate for a constellation configuration of several cube-satellites. The design will need a viewing angle better than 70 micro-radians to insure a vertical resolution around 1 kilometer as required by WMO. The final goal is a constellation of several satellites that view a region of interest from different perspectives. Such a constellation will be a perfect complement to ground observations deployed within the ARISE European infrastructure (Blanc et al. 2017) in construction.

Data availability statement. Atmospheric tide characteristics (amplitude and phase of the diurnal and semi-diurnal components) from the GSWM simulations are provided by Maura Hagan and can be downloaded freely on http://www.hao.ucar.edu/modeling/gswm/gswm.html. ERA Interim data used for estimating tidal changes can be obtained from https://apps.ecmwf.int/datasets/data/interim-full-daily/levtype=ml/.

Acknowledgments. Authors thank Adrian Simmons (ECMWF) for its support and useful discussions about the temperature requirements for ECMWF analyses. Authors thank also Jean-Francois Mahfouf (Meteo-France), Amal Chandran (Nanyang Technological University) Loren Chang (National Central University) and Pierre Tabary (CNES) for discussions about Nanosat opportunities in the domain of Earth observation. Authors thank the constructive comments of the 3 referees.

References

Baron, P., D. Murtagh, P. Eriksson, J. Mendrok, S. Ochiai, K. Pérot, H. Sagawa, and M. Suzuki, 2018: Simulation study for the stratospheric inferred winds (SIW) sub-millimeter limb sounder. *Atmospheric Measurement Techniques*, **11 (7)**, 4545–4566, doi:10.5194/amt-11-4545-2018, URL https://amt.copernicus.org/articles/11/4545/2018/.

Beig, G., and Coauthors, 2003: Review of mesospheric temperature trends. *Reviews of Geophysics*, **41**, doi:10.1029/2002RG000121.

Bertaux, J.-L., and Coauthors, 2010: Global ozone monitoring by occultation of stars: an overview of GOMOS measurements on ENVISAT. *Atmospheric Chemistry and Physics*, **10**, doi:10.5194/acp-10-12091-2010.

Bittner, M., D. Offermann, H.-H. Graef, M. Donner, and K. Hamilton, 2002: An 18-year time series of oh rotational temperatures and middle atmosphere decadal variations. *Journal of Atmospheric and Solar-Terrestrial Physics*, **64**, 1147–1166, doi:10.1016/S1364-6826(02)00065-2.

Blanc, E., and Coauthors, 2017: Toward an improved representation of middle atmospheric dynamics thanks to the ARISE project. *Surveys in Geophysics*, doi:10.1007/s10712-017-9444-0.

Chapman, S., and R. Lindzen, 1970: *Atmospheric Tides*, Vol. 10. Springer, Dordrecht, 106 pp., doi:10.1007/978-94-010-3399-2.

Charlton-Perez, A., and Coauthors, 2013: On the lack of stratospheric dynamical variability in low-top versions of the CMIP5 models. *Journal of Geophysical Research: Atmospheres*, **118**, 2494Đ2505, doi:10.1002/jgrd.50125.

Clancy, R., D. Rusch, and M. Callan, 1994: Temperature minima in the average thermal structure of the middle mesosphere (70 - 80 km) from analysis of 40- to 92-km SME global temperature profiles. *J. Geophys. Res.*, **99**, doi:10.1029/94JD01681.

Dudhia, A., S. Smith, A. Wood, and F. Taylor, 1993: Diurnal and semidiurnal temperature variability of the middle atmosphere as observed by ISAMS. *Geophys.Res.Lett.*, **20**, 1251–1254.

Farman, J., B. Gardiner, and J. Shanklin, 1985: Large losses of total ozone in Antarctica reveal seasonal ClOx/NOx interaction. *Nature*, **315**, 207–210, doi:10.1038/315207a0.

Finger, F., and W. H.M., 1967: Diurnal variation of temperature in the upper stratosphere as indicated by meteorological rocket experiment. *J. Atmos.Sci.*, **24**, 230–239.

Forbes, J. M., and D. Wu., 2006: Solar tides as revealed by measurements of mesosphere temperature by the MLS experiment on UARS. *J. Atmos.Sci.*, **63**, 1776–1797.

Funatsu, B., C. Claud, P. Keckhut, A. Hauchecorne, and T. Leblanc, 2016: Regional and seasonal stratospheric temperature trends in the last decade (2002-2014) from AMSU observations. *Journal of Geophysical Research: Atmospheres*, doi:10.1002/2015JD024305.

Funatsu, B., C. Claud, P. Keckhut, W. Steinbrecht, and A. Hauchecorne, 2011: Investigations of stratospheric temperature regional variability with lidar and Advanced Microwave Sounding unit. *Journal of Geophysical Research: Atmospheres*, **116**, doi:10.1029/2010JD014974.

Fussen, D., and Coauthors, 2019: The ALTIUS atmospheric limb sounder. *Journal of Quantitative Spectroscopy and Radiative Transfer*, **238**, 106 542, doi:https://doi.org/10.1016/j.jqsrt.2019.06.021, URL http://www.sciencedirect.com/science/article/pii/S002240731930086X.

Gelman, M., A. Miller, K. Johnson, and R. Nagatani, 1986: Detection of long-term trends in global stratospheric temperature from NMC analysis derived from NOAA satellite data. *Adv. Space Res.*, **6**, 17–26.

Gelman, M., and R. Nagatani, 1977: Objective analyses of height and temperature at the 5-, 2-, and 0.4 mb levels using meteorological rocketsonde and satellite radiation data. *Adv. Space Res.*, **XVII**, 117–122.

Haefele, A., and Coauthors, 2008: Diurnal changes in middle atmospheric h20 and o3: Observations in the Alpine region and climate models. *Journal of Geophysical Research*, **113**, doi:10.1029/2008JD009892.

Hagan, M., 1999: GSWM-98: Results for migrating solar tides. *Journal of Geophysical Research: Space Physics*, **104**, 6813–6827.

Hauchecorne, A., and M.-L. Chanin, 1980: Density and temperature profiles obtained by Lidar between 35 and 70 km. *Geophysical Research Letters*, **7**, 565–568, doi:10.1029/GL007i008p00565.

Hauchecorne, A., M.-L. Chanin, and R. Wilson, 1987: Mesospheric temperature inversion and gravity wave breaking. *Geophys. Res. Lett.*, **14**, 933–936, doi:10.1029/GL014i009p00933.

Hauchecorne, A., S. Khaykin, P. Keckhut, N. Mze, G. Angot, and C. Claud, 2019a: *Recent dynamic studies on the middle atmosphere at mid- and low-latitudes using Rayleigh Lidar and other technologies*. Springer, 757 pp.

Hauchecorne, A., and A. Maillard, 1990: A 2-D dynamical model of mesospheric temperature inversions in winter. *Geophysical Research Letters*, **17**, 2197–2200, doi:10.1029/GL017i012p02197.

Hauchecorne, A., and Coauthors, 2019b: A new MesosphEO data set of temperature profiles from 35 to 85 km using Rayleigh scattering at limb from GOMOS/ENVISAT daytime observations. *Atmospheric Measurement Techniques*, 749–761, doi:10.5194/amt-12-749-2019.

Hibbins, R., P. Espy, Y. Orsolini, V. Limpasuvan, and R. Barnes, 2019: SuperDARN observations of semidiurnal tidal variability in the MLT and the response to sudden stratospheric warming events. *Journal of Geophysical Research*, **124**, 4862–4872, doi:10.1029/2018JD030157.

Hitchman, M., and C. Leovy, 1985: Diurnal tide in the equatorial middle atmosphere as seen in LIMS temperature. *J. Atmos.Sci.*, **42**, 557–561.

Hood, L., J. Jirikowic, and M. J.P., 1993: Quasi-decadal variability of the stratosphere - influence of long-term solar ultraviolet variations. *J. Atmos. Sci.*, 3941–3958.

Hoxit, L., and R. Henry, 1973: Diurnal and annual temperature variation in the 30-60 km region as indicated by statistical analysis of rocket sonde temperature data. *J. Atmos. Sci.*, 922–933.

Huang, F., R. McPeters, P. Bhartia, H. Mayr, S. Frith, J. Russell III, and M. Mlynczak, 2010: Temperature diurnal variations (migrating tides) in the stratosphere and lower mesosphere based on measurements from SABER on TIMED. *Journal of Geophysical Research*, **115**, doi:10.1029/2009JD013698.

Kaufmann, M., and Coauthors, 2018: A highly miniaturized satellite payload based on a spatial heterodyne spectrometer for atmospheric temperature measurements in the mesosphere and lower thermosphere. *Atmospheric Measurement Techniques*, **11 (7)**, 3861–3870, doi:10.5194/amt-11-3861-2018, URL https://amt.copernicus.org/articles/11/3861/2018/.

Keckhut, P., B. Funatsu, C. Claud, and A. Hauchecorne, 2015: Tidal effects on stratospheric temperature series derived from successive Advanced Microwave Sounding units. *Quarterly Journal of the Royal Meteorological Society*, doi:10.1002/qj.2368.

Keckhut, P., and Coauthors, 1996: Semidiurnal and diurnal temperature tides (30–55 km): climatology and effect on UARS-lidar data comparison. *J. Geophys. Res. (special issue on UARS Data Validation)*, **101**, 10 299–10 310.

Keckhut, P., and Coauthors, 2010: Ozone monitoring with the GOMOS-ENVISAT experiment version 5. *Atmospheric Chemistry and Physics Discussions*, **10**, doi:10.5194/acpd-10-14713-2010.

Khaykin, S., and Coauthors, 2017a: Post-millennium changes in stratospheric temperature consistently resolved by GPS radio occultation and amsu observations: Temperature change from GPS-RO and AMSU. *Geophysical Research Letters*, doi:10.1002/2017GL074353.

Khaykin, S. M., and Coauthors, 2017b: Variability and evolution of the midlatitude stratospheric aerosol budget from 22 years of ground-based lidar and satellite observations. *Atmospheric Chemistry and Physics*, **17 (3)**, 1829–1845, doi:10.5194/acp-17-1829-2017, URL https://acp.copernicus.org/articles/17/1829/2017/.

Khaykin, S. M., and Coauthors, 2020: The 2019/20 australian wildfires generated a persistent smoke-charged vortex rising up to 35 km altitude. *Communications Earth and Environment*, **22 (1)**, 2662–4435, doi:10.1038/s43247-020-00022-5, URL https://doi.org/10.1038/s43247-020-00022-5.

Kurylo, M., 1991: Network for the detection of stratospheric change (NDSC). *Proc. SPIE*, **1491**.

Kyrola, E., and Coauthors, 2010: Retrieval of atmospheric parameters from GOMOS data. *Atmospheric Chemistry and Physics*, doi:10.5194/acp-10-11881-2010.

Lambeth, J. D., and L. Callis, 1994: Temperaturevariationsin the middle and upper stratosphere:1979-1992. *J. Geophys. Res.*, 20 701.

Le Pichon, A., and Coauthors, 2015: Comparison of co-located independent ground-based middle-atmospheric wind and temperature measurements with numerical weather prediction models. *Journal of Geophysical Research Atmospheres*, **120**, doi:10.1002/2015JD023273.

Leblanc, T., A. Hauchecorne, M.-L. Chanin, C. Rodgers, F. Taylor, and N. Livesey, 1995: Mesospheric temperature inversions as seen by ISAMS (UARS). *Geophysical Research Letters*, **22**, 1485–1488, doi:10.1029/94GL03274.

Mason, J., and Coauthors, 2017: Minxss-1 cubesat on-orbit pointing and power performance: The first flight of the Blue Canyon technologies xact 3-axis attitude determination and control system. *Journal of Small Satellites*, **6**, 651–662.

Maycock, A., and Coauthors, 2018: Revisiting the mystery of recent stratospheric temperature trends. *Geophysical Research Letters*, doi:10.1029/2018GL078035.

McLandress, C., 2002: The seasonal variation of the propagating diurnal tide in the mesosphere and lower thermosphere. part II: The role of tidal heating and zonal mean winds. *Journal of The Atmospheric Sciences*, **59**, 907–922, doi:10.1175/1520-0469(2002)059<0907:TSVOTP>2.0.CO;2.

Meftah, M., and Coauthors, 2020: UVSQ-sat, a pathfinder cubesat mission for observing essential climate variables. *Remote Sensing*, **12 (1)**, art. 92 (24 p.), doi:10.3390/rs12010092, URL https://hal-insu.archives-ouvertes.fr/insu-02424399.

Morel, B., P. Keckhut, H. Bencherif, A. Hauchecorne, G. Megie, and S. Baldy, 2004: Investigation of the tidal variations in a 3-D dynamics-chemistry-transport model of the middle atmosphere. *Journal of Atmospheric and Solar-Terrestrial Physics*, **66**, 251–265, doi:10.1016/j.jastp.2003.11.004.

Noguchi, S., Y. Kuroda, H. Mukougawa, R. Mizuta, and C. Kobayashi, 2020: Impact of satellite observations on forecasting sudden stratospheric warmings. *Geophysical Research Letters*, e2019GL086233, doi:10.1029/2019GL086233.

Oberheide, J., and O. Gusev, 2002: Observation of migrating and nonmigrating diurnal tides in the equatorial lower thermosphere. *Geophys. Res. Lett*, doi:10.1029/2002GL016213.

Raju, U. J. P., P. Keckhut, Y. Courcoux, M. Marchand, S. Bekki, B. Morel, H. Bencherif, and A. Hauchecorne, 2010: Nocturnal temperature changes over tropics during CAWSES-III campaign: Comparison with numerical models and satellite data. *Journal of Atmospheric and*

Solar-Terrestrial Physics, **72 (16)**, 1171–1179, doi:https://doi.org/10.1016/j.jastp.2010.07.013, URL http://www.sciencedirect.com/science/article/pii/S1364682610002099.

Remsberg, E., and Coauthors, 2002: An assessment of the quality of HALO temperature profiles in the mesosphere with Rayleigh backscatter lidar and inflatable falling sphere measurements. *J. Geophys. Res.*, **107**, doi:10.129/2001jD001521.

Rind, D., R. Suozzo, N. Balanchandra, and M. Prather, 1990: Climate change and the middle atmosphere: I, the doubled CO2 climate. *J. Atmos. Sci.*, 475–494.

Sheese, P., and Coauthors, 2012: Assessment of the quality of OSIRIS mesospheric temperatures using satellite and ground-based measurements. *Atmospheric Measurement Techniques*, **5**, 2993–3006, doi:10.5194/amt-5-2993-2012.

Shepherd, M., B. Reid, S. Zhang, B. Solheim, G. Shepherd, V. Wickwar, and J. Herron, 2001: Retrieval and validation of mesospheric temperatures from wind imaging interferometer observations. *Journal of Geophysical Research*, **106**, 24 813–24 830, doi:10.1029/2000JA000323.

Swinbank, R., and A. O'Neill, 1994: A stratosphere-troposphere data assimilation system. *Monthly Weather Review*, **122**, doi:10.1175/1520-0493(1994)122<0686:ASTDAS>2.0.CO;2.

Swinbank, R., R. Orris, and D. Wu, 1999: Stratospheric tides and data assimilation. *Journal of Geophysical Research*, **1041**, 16 929–16 942, doi:10.1029/1999JD900108.

Thompson, D., and Coauthors, 2012: The mystery of recent stratospheric temperature trends. *Nature*, **491**, 692–697, doi:10.1038/nature11579.

Ward, W., J. Oberheide, M. Riese, P. Preusse, and D. Offermann, 1999: Tidal signatures in temperature data from CRISTA 1 mission. *J. Geophys. Res.*, **104**, 16,391–16,403.

476 Wild, J., and Coauthors, 1995: Comparison of stratospheric temperature from several lidars using
477 NMC and MLS data as transfer reference. *Geophysical Research Letters*, **100**, 11.105–11.111.

478 Wing, R., A. Hauchecorne, P. Keckhut, S. Godin-Beekmann, S. Khaykin, and E. Mccullough, 2018:
479 Lidar temperature series in the middle atmosphere as a reference data set Ð part 2: Assessment
480 of temperature observations from MLS/AURA and SABER/TIMED satellites. *Atmospheric*
481 *Measurement Techniques*, **11**, 6703–6717, doi:10.5194/amt-11-6703-2018.

482 Wright, C., and N. Hindley, 2018: How well do stratospheric reanalyses reproduce high-resolution
483 satellite temperature measurements? *Atmospheric Chemistry and Physics*, **18**, 13 703–13 731,
484 doi:10.5194/acp-18-13703-2018.

485 Zhang, X., J. Forbes, M. Hagan, J. Russell III, S. Palo, C. Mertens, and M. Mlynczak, 2006:
486 Monthly tidal temperatures 20-120 km from TIME/SABER. *Journal of Geophysical Research*,
487 **111**, doi:10.1029/2005JA011504.

488 Zou, C.-Z., and H. Qian, 2016: Stratospheric temperature climate data record from merged
489 SSU and AMSU-A observations. *Journal of Atmospheric and Oceanic Technology*, **33**, doi:
490 10.1175/JTECH-D-16-0018.1.

LIST OF FIGURES

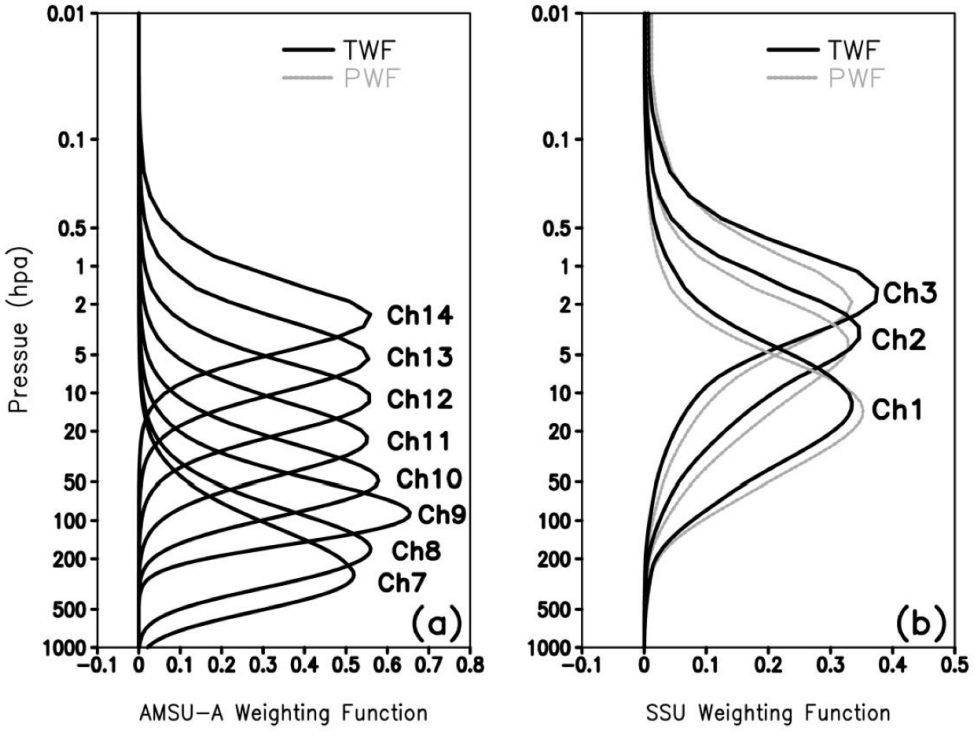

FIG. 1. Vertical weighting functions for AMSU channels 7 to 14 and for SSU from channels 1 to 3. Weighting functions estimated with Planck functions are indicated in gray (Zou and Qian 2016).

FIG. 2. Limb view showing the blue scattering induce by molecules illuminate by the sun light, the dark part above corresponding to the atmosphere, white part below corresponding to cloud and aerosols scattering (Courtesy NASA-JSC Gateway to Astronaut Photography of Earth, Image STS073-E5113).

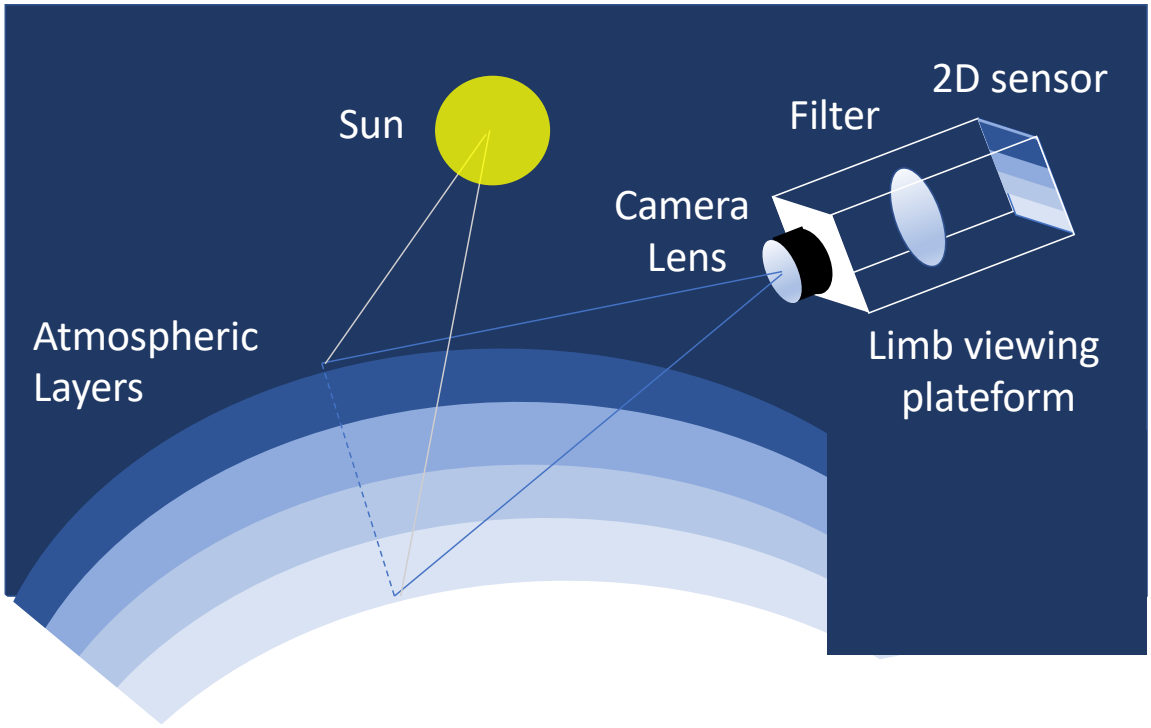

FIG. 3. Schematic instrumental setup for limb viewing geometry from space.ace.

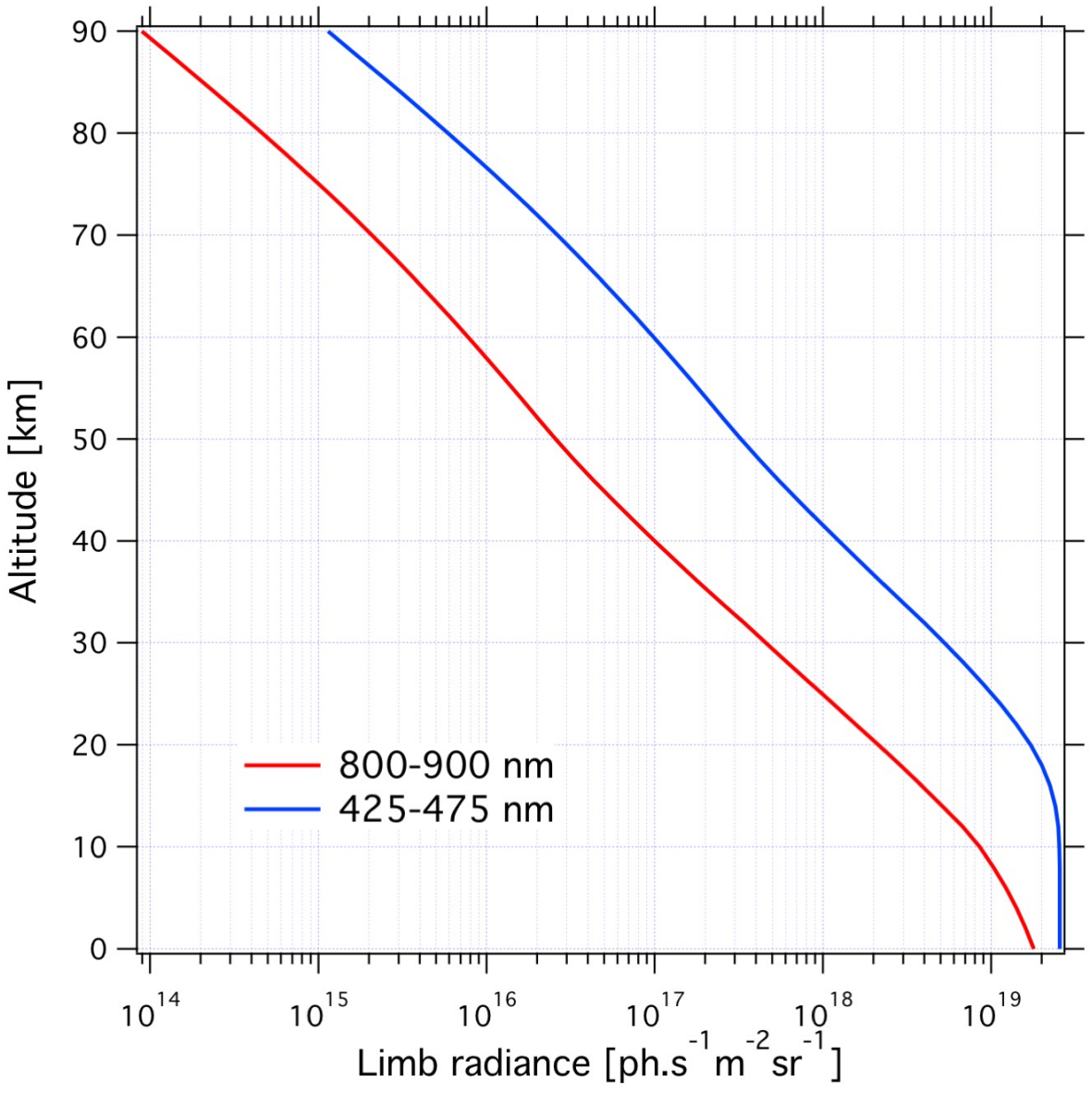

517 FIG. 4. Simulated limb radiance emission due to Rayleigh scattering in the visible domain (425-475 nm) and
518 near InfraRed domain (800-900 nm)

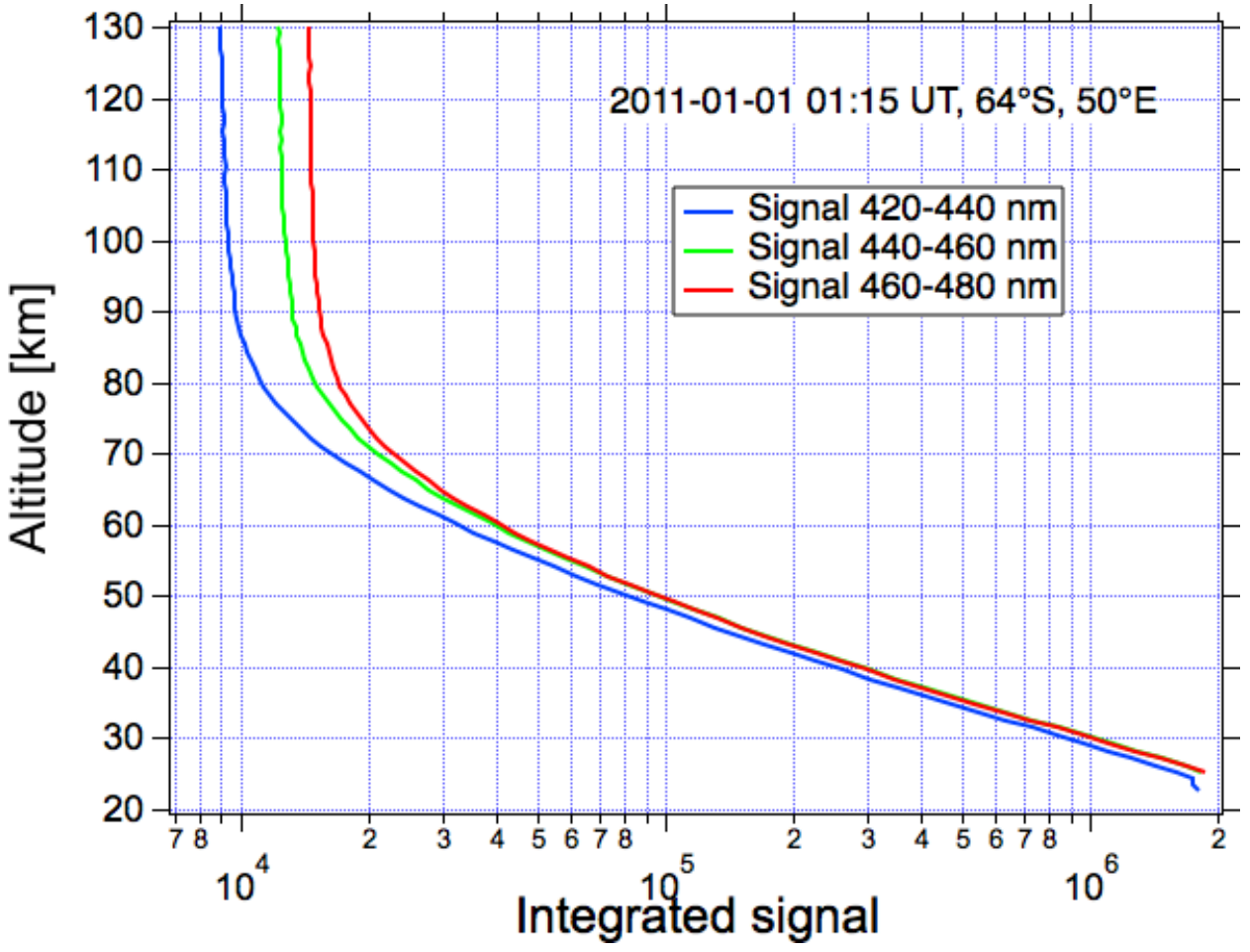

519 FIG. 5. Real observation performed by GOMOS/ENVISAT (noise detector) of the sunlight scattered by the
520 Earth's limb in 3 spectral bands as a function of tangent altitude. From Hauchecorne et al. (2019b)

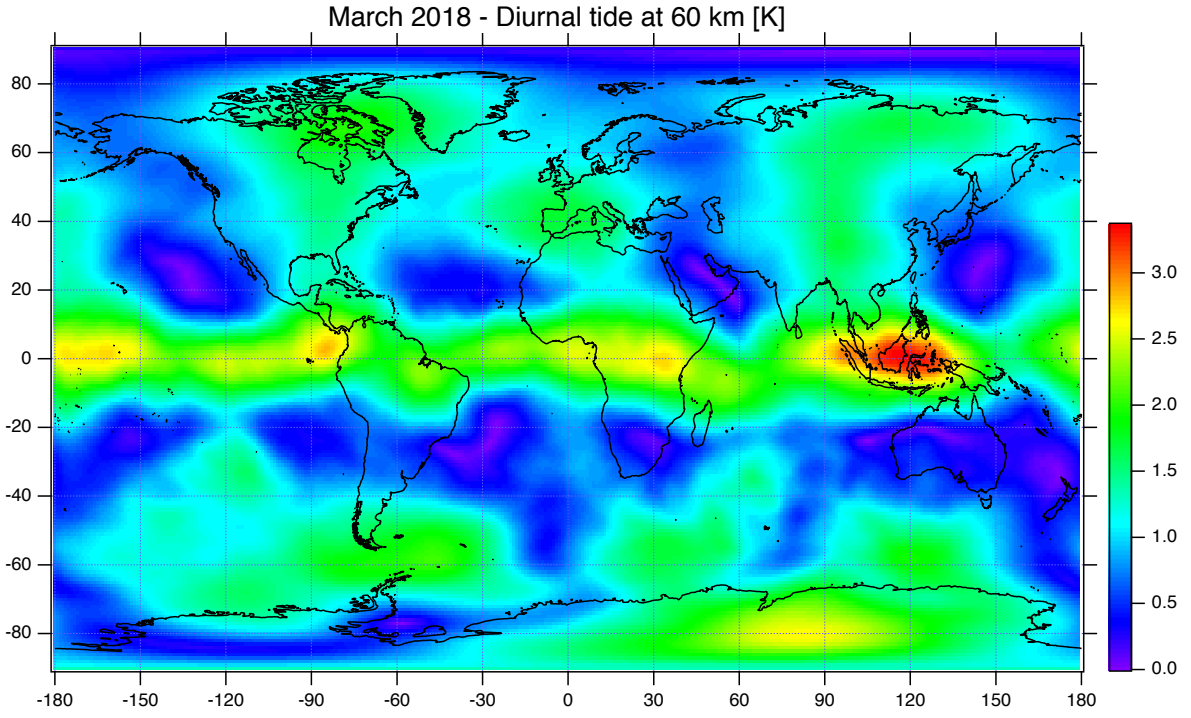

FIG. 6. Diurnal cycle derived from 6 hours ERA interim output average at 60 km over the month of March 2018.

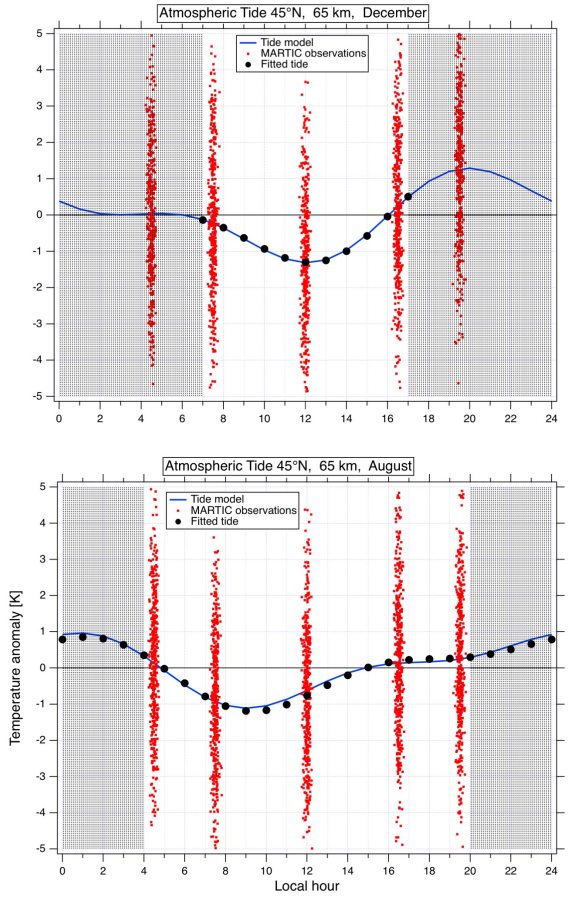

521 FIG. 7. Temperature anomalies estimated by the Global Scale Wave Model at 45°N at 65 km altitude for
522 December (a) and August (b) in Blue. Red points correspond to 30 times a temperature composed by the model
523 estimate and a random noise from a normal distribution with a standard width of 2 K for 5 different solar local
524 times. Black dots correspond to the fitted curved including 2 waves of respectively 12 and 24 hours periods and
525 a mean.